Chemical Engineering Journal 160 (2010) 302–310

Contents lists available at ScienceDirect

Chemical Engineering Journal

journal homepage: www.elsevier.com/locate/cej

Estimation of heat transfer coefficient in bubble column reactors using support vector regression

Ankit B. Gandhi, Jyeshtharaj B. Joshi*

Department of Chemical Engineering, Institute of Chemical Technology, University of Mumbai, Matunga, Mumbai 400 019, India

ARTICLE INFO

Article history:
Received 5 September 2009
Received in revised form 20 January 2010
Accepted 13 March 2010

Keywords:
Bubble column
Heat transfer coefficient
Support vector regression

ABSTRACT

The objective of this study was to develop a unified correlation for heat transfer coefficient (h) in bubble columns without internals for various gas–liquid systems using support vector regression (SVR)-based modeling technique. From the data published in open literature, 366 data points from 10 open sources spanning the years 1976–2007 for h were collected. Generalized SVR-based models have been developed for the relationship between h and prominent design and operating parameters such as column and sparger geometry, gas–liquid thermo-physical properties, operating temperature, pressure, superficial gas velocity, etc. Further, this model for h has been uploaded on the link http://www.esnips.com/web/UICT-NCL. The proposed generalized SVR-based correlations for h has prediction accuracies of 98.56% and average absolute relative error (AARE) of 7.05%. Also, the SVR-based correlation showed much improved predictions when compared with those estimated by empirical correlations in the literature.

1. Introduction

Bubble columns are extensively used in chemical, petrochemical, biochemical and metallurgical industries to carry out a variety of different unit processes such as oxidation, chlorination, alkylation, polymerization, hydrogenation, Fischer–Tropsch to synthesis, fermentation, and biological waste water treatment processes. Bubble columns are preferred in comparison to other multiphase reactors as they require less maintenance owing to absence of moving parts, offer high values of heat and mass transfer coefficients, better handling of solids and hence higher durability of solid catalyst, lesser floor space and hence are less expensive and relatively easier to operate. The present work concentrates on heat transfer study for gas–liquid contacting, whereby a discontinuous gas phase in the form of bubbles is introduced through a gas distributor situated at the bottom which then moves relative to a continuous liquid phase.

In bubble column reactors, proper design of the heat removal surfaces is crucial in order to maintain catalyst activity, reaction integrity, and product quality given that a large number of processes are highly exothermic and endothermic. Heat transfer may be in fact the most important aspect in defining performance in bubble column reactor. Therefore, it is important to understand and quantify heat transfer for optimum operation and to minimize capital costs.

Over the years, extensive experimental research on heat transfer coefficient (h) has been carried out in bubble column reactors and numerous empirical correlations have been proposed for h in various gas–liquid systems. Some of the important correlations for h for various gas–liquid systems are listed in Table 1 [1–11].

It has now been established in the literature that a large number of factors affect heat transfer coefficient (h) with each of them affecting in a different ways. For instance, h varies with a change in the size and orientation of the bubbles, which in turn is dependent on the type of sparger, gas–liquid properties, operating pressure and temperature, etc. Over the years, a large number of experiments have been reported in the literature for various gas–liquid systems and a number of system specific correlations are available. Most of these correlations are in dimensionless numbers. When the correlations constants of these correlations are carefully analyzed, they were found not to remain constant as envisaged in the correlations. For instance, the exponents on V_G, P, μ_L etc., strongly depend upon the range of all these variables and also depend upon the range of each other. As a result, all the published correlations are insufficient to meet the objectives of design engineers. For instance, Fig. 1 shows a plot of all the published correlations and deviations up to 500%. This mainly is because of the assumed constancy of empirical constants over the range considered. Besides it, these correlations loose their capability because: (i) all the important variables may not be included in the correlation (ii) if limited data are used for the development of correlation (iii) estimations are made outside the range

* Corresponding author. Tel.: +91 22 24145616/25597625; fax: +91 22 24145614.
E-mail addresses: jbjoshi@gmail.com, jb.joshi@ictmumbai.edu.in (J.B. Joshi).

1385-8947/$ – see front matter © 2010 Elsevier B.V. All rights reserved.
doi:10.1016/j.cej.2010.03.026

Nomenclature

AARE average absolute relative error $\left((1/N)\sum_{i=1}^{N}\left|(y_{predicted}-y_{experimental})/y_{experimental}\right|\right)$
C cost function
CC correlation coefficient
$\left(\sum_{i=1}^{N}(y_{experimental(i)}-y_{experimental(mean)})(y_{predicted(i)}-y_{predicted(mean)})/\sqrt{\sum_{i=1}^{N}(y_{experimental(i)}-y_{experimental(mean)})^2}\sqrt{\sum_{i=1}^{N}(y_{predicted(i)}-y_{predicted(mean)})^2}\right)$
C_{pl} specific heat of liquid (kJ/kg K)
d_B average bubble size (m)
$V_{B\infty}$ bubble rise velocity (m/s)
D column diameter (m)
d_o sparger hole diameter (m)
$f(x)$ regression function
g acceleration due to gravity (m/s^2)
H_L liquid height (m)
h heat transfer coefficient (W/m^2 K)
k thermal conductivity of liquid (W/m K)
K_d sparger distribution coefficient
N_o number of holes in the sparger
P operating pressure (kPa)
V_G superficial gas velocity (m/s)
V_L superficial liquid velocity (m/s)
y_i target output
x_i input examples (attributes)

Greek Symbols
γ gamma ($1/2\sigma^2$)
ε loss function
ϵ_G overall gas-hold-up
σ width of radial basis function (RBF) kernel
σ_W surface tension of water (N/m)
μ_L viscosity of liquid (Pa s)
σ_L surface tension of liquid (N/m)
ρ_L density of liquid (kg/m^3)
ρ_G density of gas (kg/m^3)

Subscript
G overall gas phase

Superscript
N number of training data points

of variables for which it was originally developed. In order to overcome this problem, we thought it desirable to use the technique of support vector regression (SVR). In this context, it is the objective of this study to propose a unified SVR-based data driven correlation for heat transfer coefficient (h) in bubble column reactors for various gas–liquid systems.

Data driven modeling has been finding increasing relevance and importance in chemically reacting systems. Two techniques based on data driven modeling which are gaining popularity are artificial neural networks (ANN) and support vector regression (SVR). Out of the two ANN is more commonly used. Application of ANN in context to the reactor design has been described in the literature since early

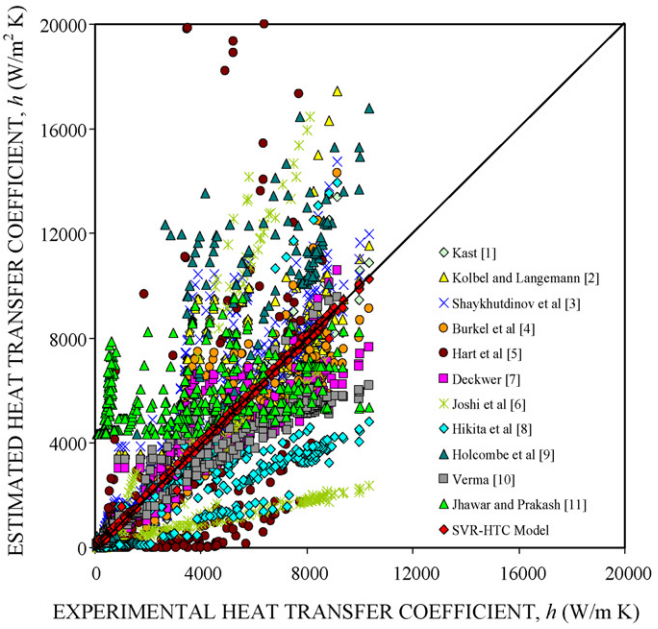

Fig. 1. Parity plot based of experimental data collected for heat transfer coefficient against the values estimated from literature correlations and SVR-based model.

nineties. For instance, Xie et al. [12] reported flow regime classification in multiphase flows using ANN, whereas Shaikh and Al-Dahhan [13] have correlated overall gas hold up in bubble column reactors using ANN. Very recently, Al-Hemiri and Ahmedzeki [14] have applied ANN for the estimation of the heat transfer coefficient in bubble columns, using a generalized model.

In this study, a unified data driven model based on support vector regression (SVR) for correlating h in bubble column reactors has been proposed. The applicability of SVR-based model in the field of chemical engineering as well as the fundamentals of SVR have been described earlier by Nandi et al. [15] and Gandhi et al. [16]. This technique is based on structural risk minimization as opposed to empirical risk minimization on which the conventional data driven techniques are based. A broad, comprehensive classification and the advantage of SVR over ANN technique has been well described elsewhere [16].

It may be pointed out that, in the present work, heat transfer study on the bubble columns is restricted only up to plain gas–liquid systems without any solids and internals within the column.

2. SVR-based modeling

The support vector regression (SVR) is an adaptation of statistical/machine learning theory known as, *support vector machines* [17]. The objective over here is to build an *epsilon*-SVR model [18] to fit a regression function, $y = f(x)$, such that it accurately predicts the outputs $\{y_i\}$ corresponding to a new set of input examples, $\{x_i\}$. In *epsilon*-SVR model, *epsilon* (ε) represents (loss function) the radius of the tube located around the regression function, $f(x)$ and the region enclosed by the tube is known as '*epsilon*-insensitive' zone. The loss function assumes a zero value in this zone and as a result it does not penalize the prediction errors with magnitudes smaller than *epsilon*. To fulfill the stated goal, SVR considers the following linear estimation function in the high dimensional feature space,

$$f(x, w) = (w \cdot \phi(x) + b) \quad (1)$$

where $\phi(x)$ = function termed *feature* and $(w \cdot \phi(x))$ the dot product in the feature space, F, such that $\phi(x) \rightarrow F$, and $w \in F$. Thus after alge-

Table 1
Summary of correlations for heat transfer coefficient for bubble column reactors.

Researcher	Gas–liquid system	Correlation
Kast [1]	Air–water	$N_{St} = 0.1\left(N_{Re}N_{Fr}N_{Pr}^{2}\right)^{-0.22}$
Kolbel and Langemann [2]	Air–water	$N_{St} = 0.124\left(N_{Re}N_{Fr}N_{Pr}^{2.5}\right)^{-0.22}$
Shaykhutdinov et al. [3]	Air–water, aq. glycerin solution	$N_{St} = 0.11\left(N_{Re}N_{Fr}N_{Pr}^{2.5}\right)^{-0.22}$
Burkel et al. [4]	Air–water, methanol, mercury	$N_{St} = 0.11\left(N_{Re}N_{Fr}N_{Pr}^{2.48}\right)^{-0.23}$
Hart et al. [5]	Air–water, ethylene glycol	$h = 0.125\left(\frac{V_G^3\rho_L}{\mu_L g}\right)^{-0.125}$
Joshi et al. [6]	Low viscosity	$\frac{hD}{k} = 0.48\left(\frac{D^{1.33}g^{0.33}(V_G-\epsilon_G V_B)^{1/3}\rho_L}{\mu_L}\right)^{0.66}\left(\frac{C_p\mu_L}{k}\right)^{0.33}$
Deckwer [7]	–	$N_{St} = 0.1\left(N_{Re}N_{Fr}N_{Pr}^{2}\right)^{-0.25}$
Hikita et al. [8]	Air-water, aq. sucrose solution, aq. methanol solution, butanol	$\frac{h}{\rho_L V_G C_p}\left(\frac{C_p\mu_L}{k}\right)^{0.66} = 0.268\left(\frac{V_G^3\rho_L}{\mu_L g}\right)^{-0.303}$
Holcombe et al. [9]	Nitrogen–water	$N_{St} = 0.1\left(N_{ReG}N_{FrG}N_{Pr}^{2}\right)^{-0.26}\exp(2.4\times10^{-4}N_{Re})$
Verma [10]	Air–water	$\frac{h}{\rho_L V_G C_p}\left(\frac{C_p\mu_L}{k}\right)^{0.5} = 0.121(1-\epsilon_G)\left(\frac{{V_G}^3\rho_L}{\mu_L g}\right)^{-0.25}$
Jhawar and Prakash [11]	Air–water	$h = 8.65\left(\frac{V_G}{\epsilon_G}\right)+1.32$ for $\frac{V_G}{\epsilon_G}\le 0.3$ m/s
		$h = 2\left(\frac{V_G}{\epsilon_G}\right)+3.3$ for $\frac{V_G}{\epsilon_G}\ge 0.3$ m/s

braic transformation the objective function (Eq. (1)), gets converted to convex optimization problem.

The primal form of the optimization problem is given as,

$$\text{Maximize}\quad \left(L(\alpha_{i,j}^{(*)}) = \sum_{i=1}^{N} y_i(\alpha_i-\alpha_i^*) - \varepsilon\sum_{i=1}^{N}(\alpha_i+\alpha_i^*)\right) - \frac{1}{2}\sum_{i=1}^{N}\sum_{j=1}^{N}(\alpha_i-\alpha_i^*)(\alpha_j-\alpha_j^*)(\phi(x_i)\cdot\phi(x_j)) \tag{2}$$

$$\text{Subject to constraints } C \ge \alpha_i, \alpha_i^* \ge 0 \text{ and } \sum_{i=1}^{N}(\alpha_i-\alpha_i^*)y_i = 0$$

where C = cost function employed to obtain a trade-off between the *flatness* of the regression function and the amount to which deviations larger than ε can be tolerated. Solving this problem (Eq. (2)) by convex quadratic programming (QP) gives the value of the coefficients α_i and α_i^*. Owing to the specific character of the above-described quadratic programming problem, only some of the coefficients, $(\alpha_i-\alpha_i^*)$, are non-zero and the corresponding input vectors, x_i, are called support vectors (SVs). These SVs are known to be as the most informative data points that compress the information content of the training set, thereby representing the entire SVR function (in a simpler case of empirical correlation these are proportionality constants and exponents over various variables). The coefficients α_i and α_i^* have an intuitive interpretation as forces pushing and pulling the regression estimate $f(x)$ towards the measurements, y_i.

Owing to this characteristic the final regression model can be defined with the help of relatively small numbers of input vectors. These SVs, x_i and the corresponding non-zero Lagrange multipliers α_i and α_i^* give the value of weight vector, w followed by the expanded form of the SVR,

$$w = \sum_{i=1}^{N}(\alpha_i-\alpha_i^*)\phi(x_i) \tag{3}$$

$$f(x,\alpha_i,\alpha_i^*) = \sum_{i=1}^{Nsv}(\alpha_i-\alpha_i^*)(\phi(x_i)\cdot\phi(x_j)) + b \tag{4}$$

However, for the aforementioned optimization problem (Eq. (2)) with an increase in the input dimensions, the dimensions in the high dimensional feature space further increases by many folds and thus becomes a computationally intractable problem. Such a problem can be overcome by defining appropriate Kernel functions in place of the dot product of the input vectors in high dimensional feature space.

$$K(x_i,x_j) = (\phi(x_i)\cdot\phi(x_j)) \tag{5}$$

The advantage of a kernel function is that the dot product in the feature space can now be computed without actually mapping the input vectors, x_i into high dimensional feature space. Thus, when using a kernel function all the necessary computations can be performed implicitly in the input space instead of in the feature space. As a consequence, the dual optimization problem (Eq. (2)) gets revised to the following form:

Maximize

$$L(\alpha_{i,j}^*) = \sum_{i=1}^{N} y_i(\alpha_i-\alpha_i^*) - \varepsilon\sum_{i=1}^{N}\left(\alpha_i+\alpha_i^*\right) - \frac{1}{2}\sum_{i=1}^{N}\sum_{j=1}^{N}(\alpha_i-\alpha_i^*)(\alpha_j-\alpha_i^*)\times K(x_i,x_j), \tag{6}$$

Subject to the following constraints:

$$C \ge \alpha_i,\ \ \alpha_i^* \ge 0 \text{ and } \sum_{i=1}^{N}(\alpha_i-\alpha_i^*)y_i = 0.$$

Thus, the basic SVR formulation takes the following form:

$$f(x,\alpha_i,\alpha_i^*) = \sum_{i=1}^{Nsv}(\alpha_i-\alpha_i^*)K(x_i,x_j) + b \tag{7}$$

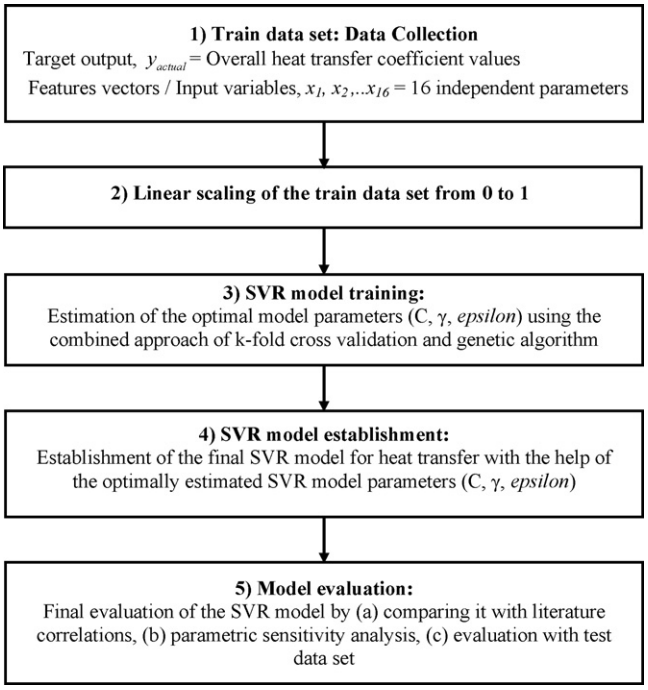

Fig. 2. Flow diagram for the establishment of the SVR-based model for heat transfer coefficient.

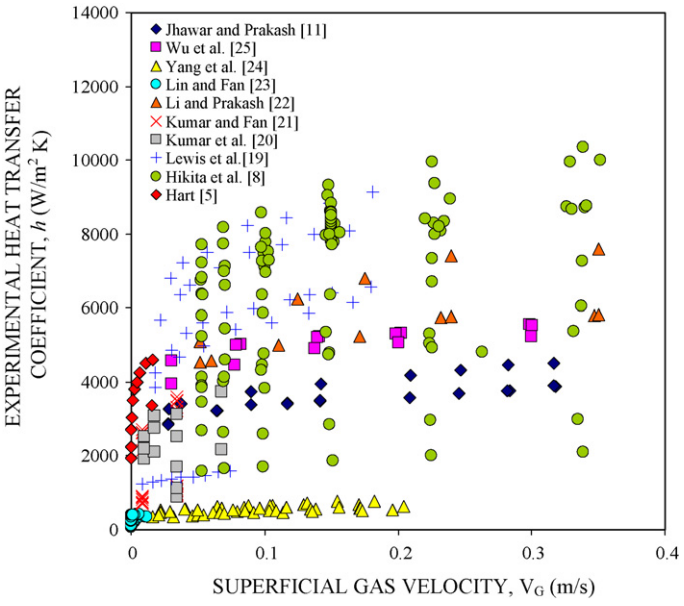

Fig. 3. Heat transfer coefficient as a function of superficial gas velocity (complete data set).

Also the bias parameter, b, can be computed by applying Karush–Kuhn–Tucker (KKT) conditions, which states that at the optimal solution the product between dual variables and constraints has to vanish. Thus giving,

$$b = \{y_i - (\alpha_i - \alpha_i^*)K(x, x_i) - \varepsilon\} \quad \text{for } \alpha_i \in \langle 0, C\rangle$$
$$b = \{y_i - (\alpha_i - \alpha_i^*)K(x, x_i) + \varepsilon\} \quad \text{for } \alpha_i^* \in \langle 0, C\rangle \tag{8}$$

where x_i and y_i, respectively, denote the ith SV and the corresponding target output. There exist several choices of kernel function K like linear, polynomial and Gaussian radial basis function. The most commonly used kernel function is the Gaussian radial basis function (RBF). It is defined as,

$$K(x_i, x_j) = \exp\left(\frac{-||x_i - x_j||^2}{2\sigma^2}\right) \tag{9}$$

where σ denotes the width of the RBF.

Further detailed mathematical description over SVR can be referred from Gandhi et al. [16].

3. Results and discussion

The approach for the development of the SVR-based correlation can be divided into three stages namely: (i) collection of data sets; (ii) calculation of the various parameters (model parameters) for establishing the regression function and (iii) model evaluation. For better understanding a flow diagram, describing the establishment of the SVR-based model for heat transfer coefficient, h is shown as Fig. 2.

3.1. Collection of data sets

All of the available data for heat transfer coefficient, h in the form published information for the last 33 years has been summarized in Table 2. All the reported measurement for h over these years has been shown in Fig. 3. From the studies carried out so far (Ref. Table 1) it can be seen that the values of h mainly depend upon the design parameters (column diameter and the sparger design), operating parameters (superficial gas and liquid velocity, temperature and pressure) and physical properties of liquid (density, surface tension, viscosity, specific heat and thermal conductivity).

Most of the studies being carried out so far have used heat flux probes to measure the heat transfer or rather, heat transfer coefficient (h). These probes are positioned either at single or multiple locations, depending upon the point of measurement of interest. Thus, they are positioned radially, either wall flushed or intruded within the column and axially at the height sufficiently off from the sparger zone (bulk region). These probes register both heat flux (q/A) and also the surface temperature (T_S) with the aid of the thermocouple as a part of the probe. On the other hand, the bulk temperature (T_b) of the fluid is being measured with the help of another thermocouple immersed within the system. The signals of heat flux and probe surface temperature are collected simultaneously at high data rate and for sufficient time interval. This helps in collecting enough number of samples (N) and thus ensuring a stable average heat transfer coefficient values (h_{avg}). The time-averaged heat transfer coefficient at a given location is being obtained by averaging the instantaneous heat transfer data and is given as,

$$h = h_{avg} = \frac{1}{N}\sum_{i=1}^{N}\frac{q/A}{T_s - T_b} \tag{10}$$

It has been observed from the studies carried out so far, that the measurement of h in some of the cases has had been at the wall (wall heat transfer coefficient), while for the rest, at the centre of the bubble column (centre heat transfer coefficient). The values of h measured at the centre of the column, are relatively higher than those measured at the column wall. The reason for this difference lies with the predominant existence of the large size, high rise velocity bubbles at the centre (relatively high turbulence zone) of the column, and small size, having low rise velocity bubbles (relatively low turbulence zone) at the column wall [11,25]. This has been explained by a direct connection of the local heat transfer coefficient to the bubble size: it increases with an increase in bubbles size, because large bubbles can create strong vortices and intense mixing in the wake region [21].

For the present study, data has been considered for both of the aforementioned cases pertaining to the measurement loca-

Table 2
Summary of the published literature for heat transfer coefficient.

Investigator	Column diameter Liquid height, m	Sparger type Hole diameter, m Number of holes	Gas–liquid system Temperature, K Pressure, kPa	Range of V_G Range of V_L (m/s)	Range of liquid properties Density, kg/m^3 Viscosity, Pa s Surface tension, N/m	Measurement location	Remarks and measurement technique
Hart [5]	0.106 0.812	Single hole 0.0063 1	Air–water 344 101.3	0.000058–0.0158 –	993 0.00038 0.0637	Centre of the column	(a) HTC measured using heat flux probe (b) No effect of column diameter, liquid height or the type of distributor seen on HTC (c) Correlation for HTC has been proposed
Hikita et al. [8]	0.10–0.19 1.45–2.30	Single hole 0.009/0.013/0.020 1	Air–water, aq., sucrose solution, aq. methanol solution and aq. butanol solution 292–318 101.3	0.05–0.35 0–0.0034	976–1230 0.0008–0.013 0.024–0.074	Wall of the column	(a) HTC measured using heat flux probe (b) Effect of liquid properties at high superficial gas velocities on HTC has been studied. (c) Correlation for HTC has been proposed
Lewis et al. [19]	0.292 1–1.5	Perforated plate 0.0019 196	Air–water, N_2–cumene 278–341 101.3	0.0087–0.18 –	965–1000 0.0001–0.0015 0.028–0.075	Centre of the column	–
Kumar et al. [20]	0.076 1.2	Sintered plate 0.00003 35,000	Air–water, aq, pentanol solution 298 101.3	0.009–0.067 0.0064–0.0137	996–997 0.00089–0.0009 0.058–0.072	Centre of the column	(a) HTC measured using heat flux probe
Kumar et al. [21]	0.0762 1.2	Single hole 0.004 1	Air–water, aq, glycerine solution 298 101.3	0.0085–0.034 0.0064–0.11	1000–1250 0.00086–0.098 0.062–0.072	Centre of the column	(a) HTC measured using heat flux probe (b) Effect of liquid viscosity on HTC has been studied.
Li and Prakash [22]	0.28 1.92	Ring sparger 0.0015 24	Air–water 296 101.3	0.035–0.35 0	1000 0.001 0.072	Centre and wall of the column	(a) HTC measured using heat flux probe (b) Effect of solid concentration on HTC has been studied.
Lin and Fan [23]	0.0508 0.64	Single nozzle 0.00158 1	N_2–paratherm 300 101.3–15,259	0.000064–0.011 0	869–882 0.032–0.038 0.025–0.029	Centre of the column	(a) HTC measured using heat flux probe (b) Effect of operating temperature and pressure on HTC has been studied. (c) Correlation for HTC has been proposed
Yang et al. [24]	0.106 1.09	Perforated plate 0.0015 120	N_2–paratherm 308–354 101.3–4200	0.06–0.21 0	864–870 0.0053–0.024 0.026–0.029	Centre of the column	(a) HTC measured using heat flux probe (b) Effect of operating temperature and pressure on HTC has been studied. (c) Correlation for HTC has been proposed.
Wu et al. [25]	0.16 1.8	Perforated plate 0.0012 163	Air–water 298 101.3–1000	0.03–0.3 0	1000 0.001 0.072	Centre and wall of the column	(a) HTC measured using heat flux probe (b) Effect of operating pressure on HTC has been studied.
Jhawar and Prakash [11]	0.15 1.05	Ring sparger and porous plate 0.000015–0.0019 20–87,000	Air–water 295 101.3	0.028–0.32 0	1000 0.001 0.072	Centre and wall of the column	(a) HTC measured using heat flux probe (b) Effect of gas sparger on HTC has been studied.

tion for heat transfer coefficient. This consideration has been done by incorporating of an additional independent parameter, known as dimensionless measurement location point (r/R) along with the other design and operating parameters. The parameter designates the radial point of measurement of the heat transfer flux (heat transfer coefficient from it) within the bubble column. For the values of h being measured at the centre of the column and at the column wall, the values of r/R are considered to be $r/R = 0$ and $r/R = 0.5$ respectively. This provision enabled us to consider the h data being measured at any radial

Table 3
Range of input and output parameters of SVR-based correlation for heat transfer coefficient.

Parameters	h (W/m^2 K)
Range of output parameters	59–14,273
Operating parameters	
Pressure, kPa	101.3–15,281
Temperature, K	278–354
Superficial gas velocity, m/s	0.000015–0.35
Superficial liquid velocity, m/s	0–0.116
Properties	
Gas	
Density, kg/m^3	1.09–170
Liquid	
Density, kg/m^3	802–1250
Viscosity, Pa s	0.0001–0.0985
Surface tension, N/m	0.022–0.0767
Thermal conductivity of liquid, W/m K	0.125–0.655
Specific heat of liquid, kJ/kg K	1.76–4.21
Reactor geometry	
Column diameter, m	0.050–0.292
Liquid height, m	0.64–2.3
Sparger type	Ring, single nozzle, multiple nozzle, perforated plate, sintered plate, spider, cross, toroidal
Sparger hole diameter, m	0.000015–0.035

location within the bubble column reactor without any discrepancy.

After careful analysis of the literature data and based on the importance and readiness in availability, following 16 independent parameters have been selected affect for the establishment of the SVR-based model for heat transfer coefficient (h): superficial gas velocity (V_G), superficial liquid velocity (V_L), sparger type (K_d), number of holes in the sparger (N_o), sparger hole diameter (d_o), dimensionless radial location of the measurement of the heat transfer coefficient (r/R), viscosity of liquid (μ_L), surface tension of liquid (σ_L), density of liquid (ρ_L), thermal conductivity of the liquid (k), specific heat of liquid (C_{pl}),gas density (ρ_G), column diameter (D), liquid height (H_L), operating pressure (P) and operating temperature (T). The ranges of parameters covered in these investigations have been covered in Table 3. It can be seen that 16 variables have been identified which control the value of heat transfer coefficient. In fact, these variables affect the average bubble size (d_B) and the bubble rise velocity ($V_{B\infty}$). These two characteristic features of the bubble columns decide the radiant profile of gas hold-up and pressure. The resulting pressure driving force generates intense liquid circulation which is upward in the central region and downwards near the column wall. The velocity gradients of mean motion and the bubble motion generate turbulence. It is known that the velocity profile and the quality of turbulence in the vicinity of the heat transfer surface govern the value of heat transfer coefficient. Further, the break-up and coalescence of bubbles also depends upon the turbulent energy dissipation rate, d_B and $V_{B\infty}$. The above subject has been discussed by Joshi and coworkers [6,26–65].

For the purpose of building comprehensive data sets for h, an extensive literature search was done spanning the years 1976–2007. The datasets for h were collected from 10 sources giving 366 experimental data points. The datasets collected were restricted to the study over gas–liquid system and without any internals within bubble column reactor.

The following additional "quality check" was also incorporated with respect to the datasets collected. In the case of manual data collection (reading the data points from the graphs of published literature), care was taken that the data was extracted from the literature with error not more than 2% in any case. This can be explained on the basis of the resolution of the 'WINDIG 2.5' software considered for the extraction of the data sets. The resolution of the software stands to be 550 × 400 pixels, constituting the total area of the plot used for the data extraction. The data from each of these plots was extracted with deviation not exceeding more than 5 × 5 pixels. Thus, maintaining the acceptable standards of data extraction error.

Table 4
Performance indicators for literature correlations for various gas–liquid systems for h.

Correlations for h	CC	AARE (%)
Kast [1]	0.82	38.78
Kolbel and Langemann [2]	0.81	34.72
Shaykhutdinov et al. [3]	0.82	45.74
Burkel et al. [4]	0.81	33.14
Hart et al. [5]	0.21	89.54
Joshi et al. [6]	0.29	71.23
Deckwer [7]	0.83	28.93
Hikita et al. [8]	0.62	63.58
Holcombe et al. [9]	0.37	64.53
Verma [10]	0.82	30.14
Jhawar and Prakash [11]	0.29	73.25
SVR (this work)	0.98	7.05

Further, the quality of the data being collected is being clearly reflected in terms of the results/predictions given by the final SVR-based model for various gas–liquid systems. After comparing the performance of the SVR-based model with the unknown test data sets (data not considered for training the model), it would be seen in the subsequent section (Section 3.5) that the SVR-based model shows substantially good agreement with the actual values of the test data set. Thus, in a way such a fine agreement between the model and the actual values shows the quality of the data being considered for training the SVR-based model for heat transfer coefficient.

3.2. Procedure for estimating regression function correlation for h

For the estimation of regression function a SVR-implementation known as '*epsilon*-SVR' in the LIBSVM software library [66] is being used to develop the SVR-based models for h. The procedure for using the LIBSVM software is being elaborately given by Gandhi et al. [16]. For the regression function developed by using the epsilon-SVR-based formalism the best values of C, epsilon and γ were obtained by using the standard k-fold cross-validation procedure [16] in combination with the genetic algorithm for stochastic grid search. The combined approach helps to find out the optimal set of the model parameters from the wide search made using genetic algorithm. The resulting optimal values of the three model parameters are $C = 207$, $\gamma = 2.54$, $epsilon = 0.0065$ for SVR-based correlation for h. Thus, for these model parameters, the corresponding numbers of support vectors were 162. Thus, the final SVR-based correlation for h gave the %AARE of 7.05% and the prediction accuracy of 98.56%. Fig. 1 is the parity showing an excellent agreement between the actual and the estimated values for the SVR-based model for h.

3.3. Comparison of the SVR-based correlation as against literature correlations

In order to check the applicability and performance of the SVR-HTC model against the literature correlations, entire dataset was subjected to the literature correlations. The simulation results for the literature correlations and SVR-based model for h are reported in Table 4. It can be seen that the SVR-based models perform much better than any of the correlations proposed in the literature by

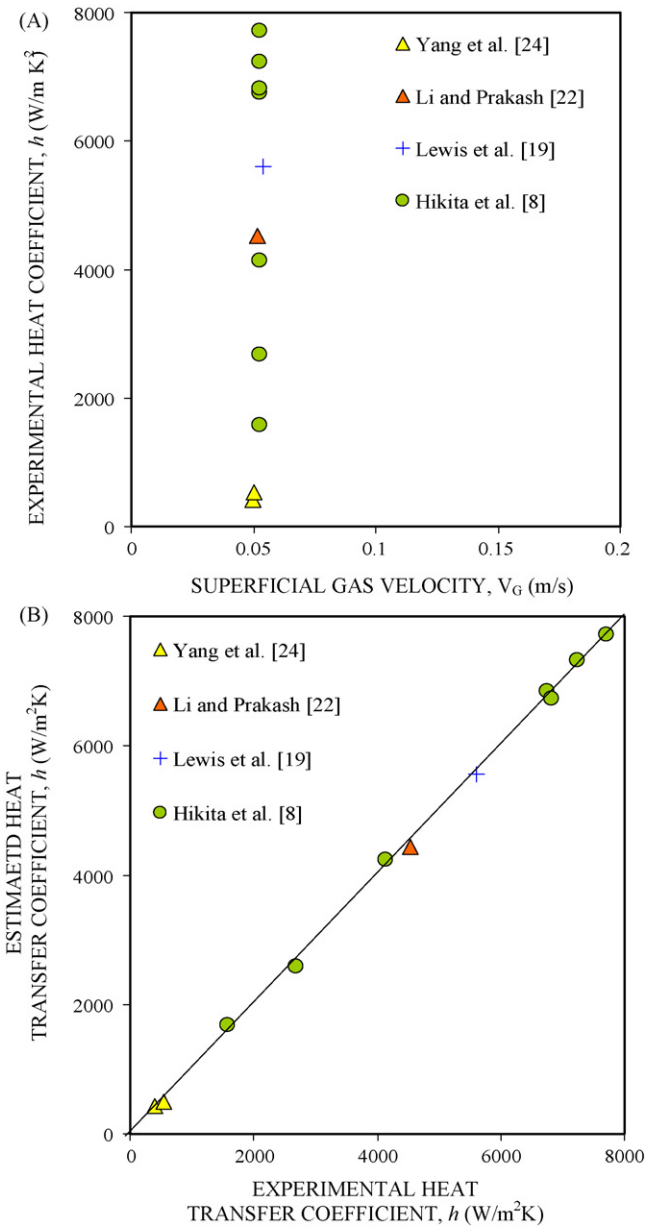

Fig. 4. Parametric sensitivity analysis for heat transfer coefficient (V_G = 0.05 m/s). (A) Heat transfer coefficient as a function of superficial gas velocity. (B) Parity plot showing the estimations by the SVR-based model.

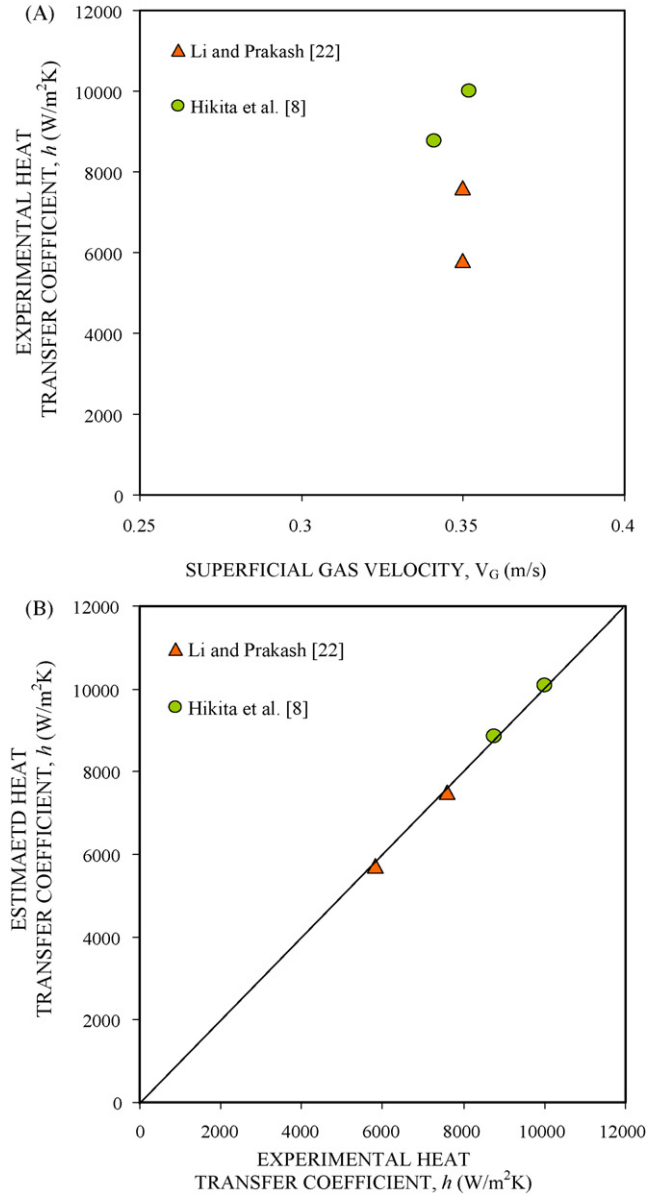

Fig. 5. Parametric sensitivity analysis for heat transfer coefficient (V_G = 0.35 m/s). (A) Heat transfer coefficient as a function of superficial gas velocity. (B) Parity plot showing the estimations by the SVR-based model.

various authors. Fig. 1 shows a comparison between the SVR-based model for h and the correlations proposed by various researchers (as mentioned within Table 1). It can be seen from Fig. 1 and the values reported in Table 4, the SVR-based models give much better correlation as compared to the various correlations reported for the available datasets.

3.4. Parametric sensitivity analysis

Parametric sensitivity analysis of the proposed model was carried out by checking the effect of the input parameters on h in bubble column reactors. Parametric sensitivity analysis involves examining the effect of individual parameters on h by the model. Thus, in order to check the effect of individual parameters on the values of h, simulations were performed at the constant gas velocity of 0.05 m/s for homogenous regime and at 0.35 m/s for heterogeneous regime. Figs. 4 and 5Figs. 4A and 5A show the existence of the various data of h with respect to superficial gas velocity for homogenous regime and the heterogeneous regime, respectively. From these figures it can be seen that, for a particular value of V_G, multiple values of h exist. This is due to the effect of individual parameters such as sparger type, number of holes in sparger, hole diameter, operating pressure and temperature, thermo physical properties of gas and liquid, column diameter, etc. on h. All the effects mentioned above are well captured by the SVR model for h as shown by the parity plot for the same as in Figs. 4B and 5B.

3.5. Performance by SVR-based correlation for test data sets

For the validation of the SVR-based model for h, it was compared against dataset not considered for training the model i.e. test data set. The simulation conditions were selected in such a manner so as to see the effect of various design and operating conditions on h. For this purpose SVR simulations were carried out using the test dataset for the system from open literature. The range of this test dataset

Table 5
Simulation conditions and results for various gas–liquid systems for *h*.

Details	SVR model for $k_L a$
Author (gas–liquid system)	Jhawar and Prakash [11] (air–water)
Pressure, kPa	101.32
Temperature, K	295
Superficial gas velocity, m/s	0.028–0.31
Superficial liquid velocity, m/s	0
Gas density, kg/m^3	1.18
Liquid density, kg/m^3	1000
Liquid viscosity, Pa s	0.001
Liquid surface tension, N/m	0.0728
Thermal conductivity of liquid, W/m K	0.595
Specific heat of liquid, kJ/kg K	4.18
Column diameter, m	0.15
Liquid height, m	1.05
Sparger type	Ring sparger
Number of sparger holes	20
Sparger hole diameter, m	0.0019
Correlation coefficient, CC	0.99
% AARE	4.79

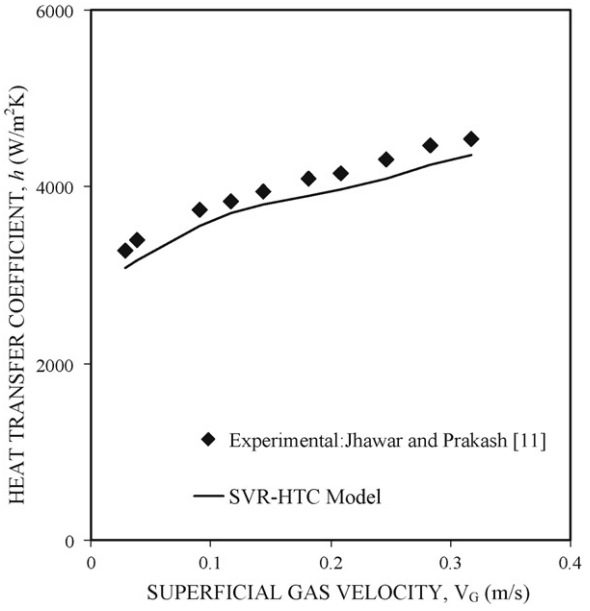

Fig. 6. Estimations made by SVR-based model for *h* for the experimental conditions of Jhawar and Prakash [11].

along with the performance of the SVR-based model is reported in Table 5. The *h* simulations were carried out at experimental conditions of Jhawar and Prakash [11]. The effect of change in the column diameter and sparger type onto the *h* values has been well reflected by SVR model. Fig. 6 qualitatively shows the estimation made by the SVR-based model for *h* for the test input data set.

3.6. Web based SVR models for h

Since, the numbers of support vectors are large in number (162) for the SVR-based model for *h*, they are made available on the web. For this purpose a SVR simulation tool was prepared and made available on the web for the estimation of *h* for bubble column reactors. This tool is named as 'SVR_HTC_BC' and can be downloaded from the web link http://www.esnips.com/web/UICT-NCL. This tool is in the form of a Microsoft excel sheet wherein the sheet of interest is named as '*SVR model htc*'. Here one can insert the desired input features (16) and the cell named '*predicted heat transfer coefficient*' gives the value of the estimated output (*h*). The estimation is made on the basis of the procedure described in the earlier sections. The support vectors are listed in their scaled format in the sheet named '*support vectors htc*'. The calculation of kernel elements is done in a sheet named '*kernel elements htc*'. The above-mentioned sheet is password protected in order to ensure that they are not tampered with as the sheet possesses vital information for the model. The summation of the product of the above-mentioned kernel elements and the corresponding non-zero Lagrange multipliers for each of the support vectors with addition of the bias term to it give the predicted output. This estimation is shown in the cell named '*predicted heat transfer coefficient*' in sheet '*SVR model htc*'.

4. Conclusion

(1) In the case of bubble columns, all the published correlations (10) for heat transfer coefficient (*h*) have been analyzed. A critical assessment has been made regarding their predictive capability as shown in Fig. 1. It has been shown that the published correlations has four limitations (a) all the governing parameters are not considered, (b) datasets have been selected over a limited range of parameters, (c) a procedure was needed for confirming the quality of datasets used for developing the correlations, (d) all the published correlations do not consider the interdependence of parameters on *h*.
(2) The estimation made by the SVR-based correlation for *h* shows remarkable improvement for bubble column reactors as compared to the other types of empirical and semi-empirical correlations available in the literature. The generalized SVR-based correlation for the estimation of *h* yield AARE of 7.05% and prediction accuracy of 98.56%, which is far better than those obtained through the selected literature correlations.
(3) The SVR-based correlation for *h* gave enhanced and more accurate predictions for a variety of gas–liquid systems over a wide range of operating pressures, operating temperatures, superficial gas and liquid velocities and various column diameters and liquid heights. Hence the proposed SVR-based correlation is expected to be useful in the design and scale-up of bubble column reactors.
(4) We have provided the SVR-based correlation for *h* on the website (http://www.esnips.com/web/UICT-NCL). We invite the users to communicate the deviations which will enable to improvise the data driven model.

Acknowledgements

AG thanks the financial support under the J.C. Bose Fellow (J.B. Joshi), Department of Science and Technology, Govt. of India.

Appendix A. Supplementary data

Supplementary data associated with this article can be found, in the online version, at doi:10.1016/j.cej.2010.03.026.

References

[1] W. Kast, Analyse des warmeubergangs in blasensaulen, Int. J. Heat Mass Transfer (1962) 329–336.
[2] H. Kölbel, H. Langemann, Warmeubergang in blasensaulen, Erdoel Zeitschrift 80 (1964) 405–415.
[3] A.G. Shaykhutdinov, N.U. Bakirov, A.G. Usmanov, Determination and mathematical correlation of heat transfer coefficients under conditions of bubble flow, cellular, and turbulent foam, Int. J. Chem. Reactor Eng. 11 (1971) 641–645.
[4] W. Burkel, Der wärmeübergang an heiz- und kühlflächen in begasten flüssigkeiten (Heat transfer at heating and cooling surfaces in gassed liquids), Chem. Eng. Technol. 44 (1972) 265–268.
[5] W.F. Hart, Heat transfer in bubble-agitated systems. A general correlation, Ind. Eng. Chem. Res. 15 (1976) 109–114.
[6] J.B. Joshi, M.M. Sharma, Y.T. Shah, C.P.P. Singh, M. Ally, G.E. Klinzing, Heat transfer in multiphase contactors, Chem. Eng. Commun. 6 (1980) 257–271.

[7] W.D. Deckwer, On the mechanism of heat transfer in bubble column reactors, Chem. Eng. Sci. 35. (1980) 1341–1365.
[8] H. Hikita, S. Asai, H. Kikukawa, T. Zaike, M. Ohue, Heat transfer coefficient in bubble columns, Ind. Eng. Chem. Res. 20 (1981) 540–545.
[9] N.T. Holcombe, D.N. Smith, H.N. Knickle, W. O'Dowd, Thermal dispersion and heat transfer in nonisothermal bubble columns, Chem. Eng. Commun. 21 (1983) 135–150.
[10] A.K. Verma, Heat transfer mechanism in bubble columns, Chem. Eng. J. 42 (1989) 205–208.
[11] A.K. Jhawar, A. Prakash, Analysis of local heat transfer and hydrodynamics in a bubble column using fast response probes, Chem. Eng. Sci. 62 (2007) 7274–7281.
[12] T. Xie, S.M. Ghiaasiaan, S. Karrila, Artificial neural network approach for flow regime classification in gas–liquid fiber flows based on frequency domain analysis of pressure signals, Chem. Eng. Sci. 59 (2004) 2241–2251.
[13] A. Shaikh, M. Al-Dahhan, Development of an artificial neural network correlation for prediction of overall gas-holdup in bubble column reactors, Chem. Eng. Process. 42 (2003) 599–610.
[14] A.A. Al-Hemiri, N.S. Ahmedzeki, Prediction of the heat transfer coefficient in a bubble column using an artificial neural network, Int. J. Chem. Reactor Eng. 6 (2008) A72.
[15] S. Nandi, Y. Badhe, J. Lonari, U. Sridevi, B.S. Rao, S.S. Tambe, B.D. Kulkarni, Hybrid process modeling and optimization strategies integrating neural networks/support vector regression and genetic algorithms: study of benzene isopropylation on hbeta catalyst, Chem. Eng. J. 97 (2004) 115–129.
[16] A.B. Gandhi, J.B. Joshi, V.K. Jayaraman, B.D. Kulkarni, Development of support vector regression (SVR)-based correlation for prediction of overall gas hold-up in bubble column reactors for various gas–liquid systems, Chem. Eng. Sci. 62 (2007) 7078–7089.
[17] V. Vapnik, S. Golowich, A.J. Smola, Support vector method for function approximation, regression estimation and signal processing, Adv. Neural Info. Process. Syst. 9 (1996) 281–287.
[18] S.R. Gunn, Support vector machines for classification and regression, Technical report, Department of Electronics and Computer Science. University of Southampton, 1998 (http://trevinca.ei.uvigo.es/~cernadas/tc03/mc/SVM.pdf).
[19] D.A. Lewis, R.W. Field, A.M. Xavier, D. Edwards, Heat transfer in bubble columns, Trans. Inst. Chem. Eng. 60 (1982) 40–47.
[20] S. Kumar, K. Kusakabe, L.S. Fan, Heat transfer in three-phase fluidization and bubble-columns with high gas holdups, AIChE J. 39 (1993) 1399–1405.
[21] S. Kumar, L.S. Fan, Heat-transfer characteristics in viscous gas–gas–liquid–solid systems, AIChE J. 40 (1994) 745–755.
[22] H. Li, A. Prakash, Heat transfer and hydrodynamics in a three-phase slurry bubble column, Ind. Eng. Chem. Res. 36 (1997) 4688–4694.
[23] T.-J. Lin, L.-S. Fan, Heat transfer and bubble characteristics from a nozzle in high-pressure bubble columns, Chem. Eng. Sci. 54 (1999) 4853–4859.
[24] G.Q. Yang, X. Luo, L.S. Fan, Heat-transfer characteristics in slurry bubble columns at elevated pressures and temperatures, Ind. Eng. Chem. Res. 39 (2000) 2568–2577.
[25] C. Wu, M.H. Al-Dahhan, A. Prakash, Heat transfer coefficients in a high pressure bubble column, Chem. Eng. Sci. 62 (2007) 140–147.
[26] J.B. Joshi, M.M. Sharma, Mass transfer characteristics of horizontal sparged contactors, Trans. Inst. Chem. Eng. (U.K.) 54 (1976) 42–53.
[27] J.B. Joshi, M.M. Sharma, A circulation cell model for bubble columns, Trans. Inst. Chem. Eng. (U.K.) 57 (1979) 244–251.
[28] A.B. Pandit, J.B. Joshi, Mixing in mechanically agitated contactors bubble columns and modified bubble columns, Chem. Eng. Sci. 38 (1983) 1189–1215.
[29] J.B. Joshi, Solid–liquid-fluidised beds – some design aspects, Trans. Inst. Chem. Eng. (U. K.). A: Chem. Eng. Res. Des. 61 (1983) 143–161.
[30] V.K. Patil, J.B. Joshi, M.M. Sharma, Sectionalised bubble column: gas hold-up & wall side solid–liquid mass transfer coefficient, Can. J. Chem. Eng. 62 (1984) 228–232.
[31] A.B. Pandit, J.B. Joshi, Mass and heat transfer characteristics of three phase sparged reactors, Trans. Inst. Chem. Eng. (U.K.) – A: Chem. Eng. Res. Des. 64 (1986) 125–157.
[32] J.B. Joshi, V.V. Ranade, V.V. Gharat, S.S. Lele, Sparged loop reactors, Can. J. Chem. Eng. 68 (1990) 705–741.
[33] J.B. Joshi, Comments on flow mapping in bubble columns using CARPT, Chem. Eng. Sci. 46 (1992) 508–509.
[34] S.D. Gharat, J.B. Joshi, Transport phenomena in bubble column reactors-I: flow pattern, Chem. Eng. J. 48 (1992) 141–151.
[35] S.D. Gharat, J.B. Joshi, Transport phenomena in bubble column reactors-II: pressure drop, Chem. Eng. J. 48 (1992) 153–166.
[36] N.S. Deshpande, M. Dinakar, J.B. Joshi, Disengagement of the gas phase in bubble columns, Int. J. Multiphase Flow 21 (1995) 1191–1201.
[37] B.N. Thorat, A.V. Shevade, K.R. Bhilegaonkar, R.H. Agalave, Parasu Veera, U.S.S. Thakre, A.B. Pandit, S.B. Sawant, J.B. Joshi, Effect of sparger design and height to diameter ratio on gas hold-up in bubble column reactors, Trans. Inst. Chem. Eng. A: Chem. Eng. Res. Des. 76 (1998) 823–834.
[38] U. Parasu Veera, J.B. Joshi, Hold-up profiles by tomography: effect of sparger design and height of dispersion in bubble columns, Trans. Inst. Chem. Eng. 77 (1999) 303–317.
[39] S.S. Thakre, J.B. Joshi, CFD simulation of flow in bubble column reactors importance of drag force formulation, Chem. Eng. Sci. 54 (1999) 5055–5060.
[40] S.S. Thakre, J.B. Joshi, CFD modeling of heat transfer in turbulent pipe flow A, Chem. Eng. J. 54 (2000) 5055–5060.
[41] U. Parasu Veera, J.B. Joshi, Measurement of gas hold-up profiles in bubble column by gamma ray tomography: effect of liquid phase properties, Trans. Inst. Chem. Eng. 78A (2000) 425–434.
[42] J.B. Joshi, Computational flow modelling and design of bubble column reactors, Chem. Eng. Sci. 56 (2001) 5893–5933.
[43] J.B. Joshi, V.S. Vitankar, A.A. Kulkarni, M.T. Dhotre, K. Ekambara, Coherent flow structures in bubble column reactors, Chem. Eng. Sci. 57 (2002) 3157–3183.
[44] S.S. Thakre, J.B. Joshi, Momentum mass and heat transfer in single phase turbulent flow, Rev. Chem. Eng. 18 (2002) 83–293.
[45] M.T. Dhotre, J.B. Joshi, CFD simulation of gas chamber for gas distributor design, Can. J. Chem. Eng. 81 (2003) 677–683.
[46] M.T. Dhotre, K. Ekambara, J.B. Joshi, CFD simulation of sparger design and height to diameter ratio on gas hold-up profiles in bubble column reactors, Exp. Therm. & Fluid Sci. 28 (2004) 407–421.
[47] M.T. Dhotre, J.B. Joshi, CFD simulation of heat transfer in turbulent pipe flows, Ind. Eng. Chem. Res. 43 (2004) 2816–2829.
[48] M.T. Dhotre, J.B. Joshi, Two dimensional CFD model for flow pattern heat transfer and pressure drop in bubble column reactor, Trans. Inst. Chem. Eng.: Chem. Eng. Res. Des. 82 (A6) (2004) 689–707.
[49] O. Lorenz, A. Schumpe, K. Ekambara, J.B. Joshi, Liquid phase axial mixing in bubble columns operated at high pressures, Chem. Eng. Sci. 60 (2005) 3573–3586.
[50] A.A. Kulkarni, J.B. Joshi, Bubble formation and bubble rise velocity in gas–liquid systems: a review, Ind. Eng. Chem. Res. 44 (2005) 5873–5931.
[51] M.T. Dhotre, V.S. Vitankar, J.B. Joshi, CFD simulation of steady state heat transfer in bubble column, Chem. Eng. J. 108 (2005) 117–125.
[52] A.V. Kulkarni, J.B. Joshi, Estimation of hydrodynamic and heat transfer characteristics of bubble column by analysis of wall pressure measurements and CFD simulations, Trans. Inst. Chem. Eng. A: Chem. Eng. Res. Des. 84 (2006) 601–609.
[53] M.R. Bhole, S. Roy, J.B. Joshi, LDA measurements in bubble column: effect of sparger, Ind. Eng. Chem. Res. 45 (2006) 9201–9207.
[54] M.T. Dhotre, J.B. Joshi, Design of a gas distributor: three-dimensional CFD simulation of a coupled system consisting of a gas chamber and a bubble column, Chem. Eng. J. 125 (2006) 149–163.
[55] A.A. Kulkarni, K. Ekambara, J.B. Joshi, On the development of flow pattern in a bubble column reactor: experiments and CFD, Chem. Eng. Sci. 62 (2007) 1049–1079.
[56] M.R. Bhole, J.B. Joshi, D. Ramakrishna, Population balance modeling for bubble column operating in the homogeneous regime, AIChE J. 53 (2007) 750–756.
[57] A.V. Kulkarni, S. Roy, J.B. Joshi, Pressure and flow distribution in pipe and ring sparger: experimental measurements and CFD simulation, Chem. Eng. J. 133 (2007) 173–186.
[58] C.S. Mathpati, J.B. Joshi, Insight into theories of heat and mass transfer at the solid–fluid interface using direct numerical simulation and large eddy simulation, Ind. Eng. Chem. Res. 46 (2007) 8525–8557.
[59] M.R. Bhole, J.B. Joshi, D. Ramkrishna, CFD simulation of bubble columns incorporating population balance modeling, Chem. Eng. Sci. 63 (2008) 2267–2282.
[60] M.V. Tabib, S.V. Roy, J.B. Joshi, CFD simulation of bubble column: an analysis of interphase force and turbulence models, Chem. Eng. J. 139 (2008) 589–614.
[61] S.S. Gulawani, S.K. Dahikar, C.S. Mathpati, J.B. Joshi, M.S. Shah, C.S. RamaPrasad, D.S. Shukla, Analysis of flow pattern and heat transfer in direct contact condensation, Chem. Eng. Sci. 64 (2009) 1719–1738.
[62] S.S. Deshpnade, C.S. Mathpati, S.S. Gulawani, J.B. Joshi, V. Ravi Kumar, Effect of flow structures on heat transfer in single and multiphase jet reactors, Ind. Eng. Chem. Res. 48 (2009) 9424–9440.
[63] J.B. Joshi, M.V. Tabib, S.S. Desphande, C.S. Mathpati, Dynamics of flow structures and transport phenomena. 1. Experimental and numerical techniques for identification and energy content of flow structures, Ind. Eng. Chem. Res. 48 (2009) 8244–8284.
[64] C.S. Mathpati, M.V. Tabib, S.S. Desphande, J.B. Joshi, Dynamics of flow structures and transport phenomena. 2. Relationship with design objectives and design optimization, Ind. Eng. Chem. Res. 48 (2009) 8285–8311.
[65] A.A. Ganguli, A.B. Pandit, J.B. Joshi, CFD simulation of heat transfer in a two-dimensional vertical enclosure, Trans. Inst. Chem. Eng. A: Chem. Eng. Res. Des. 87 (2008) 711–727.
[66] C.-C. Chang, C.-J. Lin, LIBSVM: A Library for Support Vector Machines, 2001. Software available at http://www.csie.ntu.edu.tw/~cjlin/libsvm.